

Review

# An Overview of Radiation Induced Deep Level Defects in n-type 4H-SiC Studied by Junction Spectroscopy Techniques

Ivana Capan

Ruder Boskovic Institute, Bijenička 54, 10 000 Zagreb, Croatia  
capan@irb.hr

**Abstract:** In this review paper, an overview of radiation induced deep level defects in n-type 4H-SiC studied by junction spectroscopy techniques, is given. In addition to carbon vacancy ( $V_c$ ), present in as-grown material already, we focus on the following deep level defects: silicon vacancy ( $V_{Si}$ ), carbon interstitial ( $C_i$ ), and carbon antisite-carbon vacancy ( $C_{Si}-V_c$ ) pair. Recent advances in measurements by junction spectroscopy techniques that have led the progress toward better understanding of radiation induced defects are presented.

**Keywords:** 4H-SiC; defects; radiation, DLTS.

## 1. Introduction

Silicon carbide (SiC) is a wide bandgap semiconductor suitable for high temperature and high-power applications. We are witnessing a rapid growth in number of applications for SiC-based devices such as PiN diodes, and MOSFETs in the past few years. Moreover, SiC has attracted a lot of attention as point-like defects which are introduced by ion implantation or proton irradiation in a deterministic way, such as  $V_{Si}$ , are considered as promising candidates for quantum computing and sensing [1].

Table 1. Parameters for SiC polytypes [2].

SiC Poly-type	Energy band gap (eV)	Electron mobility $\parallel / \perp$ to c-axis ( $\text{cm}^2\text{V}^{-1}\text{s}^{-1}$ )	Hole mobility ( $\text{cm}^2\text{V}^{-1}\text{s}^{-1}$ )	Electric field $\parallel$ to c-axis (MV/cm)	Thermal conductivity ( $\text{W cm}^{-1}\text{K}^{-1}$ )
4H	3.26	1200/1020	120	2.8	3.3-4.9
6H	3.02	100/450	100	3.0	3.3-4.9
3C	2.36	~1000/1000	100	1.4	3.3-4.9

Among all SiC polytypes, 4H is the most studied. It has the largest bandgap of 3.23 eV. More parameters are given in Table 1. Due to the high and isotropic mobility of carriers, the 4H polytype of SiC is preferred as material for power electronics [2], bipolar devices [3], quantum computing [1], and radiation detection devices [4].

Wide-spread applicability of 4H-SiC material for electronic devices was mostly hindered by trapping/recombination of carriers and compensation effects due to electrically

active deep level defects. Electrically active deep level defects act as traps for charge carriers, and therefore influence electrical properties of electronic device and cause a deterioration of device performance. We will focus on n-type 4H-SiC material, as it is the preferred type of material for the electronic devices.

In this review, we provide an overview of electrically active deep level defects in n-type 4H-SiC material. Since we are covering the electrically active defects, the primary experimental techniques to be included are junction spectroscopy techniques. Junction spectroscopy technique is a term describing measurements performed on a semiconductor junction using electrical or electro-optical techniques [5]. The role of the junction is to create a depletion region (for example Schottky or p-n diode), as its usage brings the important advantage over other bulk techniques. The advantage is that it is much easier to manipulate the occupancy of defects producing energy levels in the bandgap (i.e., deep level defects) within the depletion region than in bulk [5]. The most common junction spectroscopy technique is the deep level transient spectroscopy (DLTS). DLTS is one of the most sensitive methods for determination of electronic properties of deep level defects in semiconductors. DLTS can detect deep level defects in concentration around  $10^{10} \text{ cm}^{-3}$  [5]. It provides information regarding the activation energy for electron/hole emission, capture cross-section, and concentration/density of defects. However, the main DLTS deficiency is the lack in energy resolution i.e., it is almost impossible to resolve two closely spaced deep energy levels. The improvement came in another junction spectroscopy technique and brought an order of magnitude better energy resolution. This technique is called Laplace DLTS (L-DLTS) [5]. The list of other junction spectroscopy techniques includes, but it is not limited to isothermal DLTS and minority carrier transient spectroscopy (MCTS). The isothermal DLTS has proven as a very useful technique for studying the bi-stable defects in n-type 4H-SiC [6], while MCTS gives information on minority carrier traps. Minority carriers could be optically generated by use of above-bandgap light [7].

Although we will focus on DLTS results in this review, results obtained with other techniques such as electron paramagnetic resonance (EPR) and photoluminescence (PL), will not be excluded. However, it should be noted that direct comparison of DLTS and EPR is difficult or impossible in some cases. The reason is, DLTS is usually used for measuring deep level defects in concentrations which are a few orders of magnitude below the detection limit of EPR.

Recent advances in measuring and identifying deep level defects in 4H-SiC have resulted in numerous reported studies and huge amount of the available data. It has become difficult to follow all these advances and stay updated. Different defects labeling used for the same defects has also brought a certain confusion.

The main aim of this review is to provide updates results on the radiation induced deep level defects in n-type 4H-SiC. Here, we have focused on recent advances, and studies reported in the past few years. Therefore, we highly recommend to our readers to look for more details in provided references and references within.

## 2. Deep level defects in n-type 4H-SiC

For many years researchers within the SiC community, in particular researchers working with DLTS, have reported studies on deep level defects in 4H-SiC and used different labelling for defects identification. As a result, we have had different “families” of defects, known as S1-S4 [1,8, 9], RD1-4 [10], ET1-2 [11,12] EH3-7 [13,14] etc. Recently, one “family” has prevailed, and it is becoming a standard notation.

They are:  $Z_{1/2}$ ,  $\text{EH}_{6/7}$ ,  $S_{1/2}$ ,  $\text{EH}_{1/3}$ , and  $\text{EH}_{4/5}$ . Based on the recent results obtained by DLTS, L-DLTS, and EPR measurements, combined with the density functional calculations (DFT), above mentioned deep level defects are identified as: acceptor and donor state of the carbon vacancy ( $V_c$ ) [15], silicon vacancy ( $V_{\text{Si}}$ ) [1], carbon interstitial ( $C_i$ ) [13], and carbon antisite-carbon vacancy ( $C_{\text{Si}}-V_c$ ) pair [14], respectively.

Figure 1. shows a schematic energy bandgap diagram of the n-type 4H-SiC with the most common deep level defects. It should be noted that diagram is prepared based only on DLTS measurements; therefore  $Z_{1/2}$  and  $EH_{6/7}$  are represented as single levels. Recent advances in separating the signals arising from the  $Z_1$  and  $Z_2$ , and  $EH_6$  and  $EH_7$  by means of L-DLTS will be thoroughly explained later in the text.

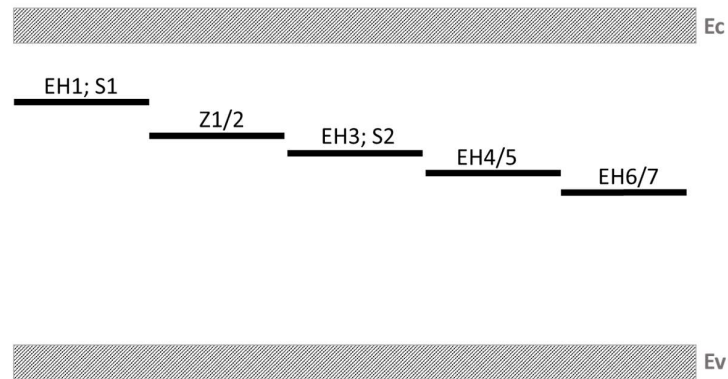


Figure 1. Schematic energy bandgap diagram for the n-type 4H-SiC, with the most common deep level defects.

Figure 1. clearly shows how closely spaced are all the above-mentioned deep level defects. In fact,  $EH_{1/3}$  and  $S_{1/2}$ , have the identical activation energies for electron emissions, 0.40 and 0.70 eV. Such unusual behavior has led to confusion not only in labelling but also in distinguishing these deep level defects. Table 2. provides details on the deep level defects covered in this paper.

Table 2. List of all deep level defects in n-type 4H-SiC covered in this review paper. Information about defects labelling, identification, activation energy and references are listed.

Label	Identification	Activation energy (eV)	References
EH <sub>1</sub>	C <sub>i</sub>	0.40	[13,16]
EH <sub>3</sub>	C <sub>i</sub>	0.70	[13,16]
S <sub>1</sub>	V <sub>Si</sub> (-3/-)	0.40	[1, 8, 17, 18]
S <sub>2</sub>	V <sub>Si</sub> (=/-)	0.70	[1, 8, 17, 18]
Z <sub>1</sub>	V <sub>c</sub> (=0)	0.59	[15, 19, 20]
Z <sub>2</sub>	V <sub>c</sub> (=0)	0.67	[15, 19, 20]
EH <sub>4/5</sub>	C <sub>Si</sub> -V <sub>c</sub> (+/0)	1.0 – 1.1	[14, 21]

EH <sub>6</sub>	V <sub>c</sub> (0/++)	1.30	[15, 22, 23]
EH <sub>7</sub>	V <sub>c</sub> (0/++)	1.40	[15, 22, 23]

### 3.1. Carbon vacancy

Figure 2 shows typical DLTS spectrum for the as-grown n-type 4H-SiC sample. Two peaks, Z<sub>1/2</sub> (maximum at around 300 K) and EH<sub>6/7</sub> (maximum at around 650 K) are observed. The estimated activation energies for electron emission are 0.67 and 1.74 eV, respectively.

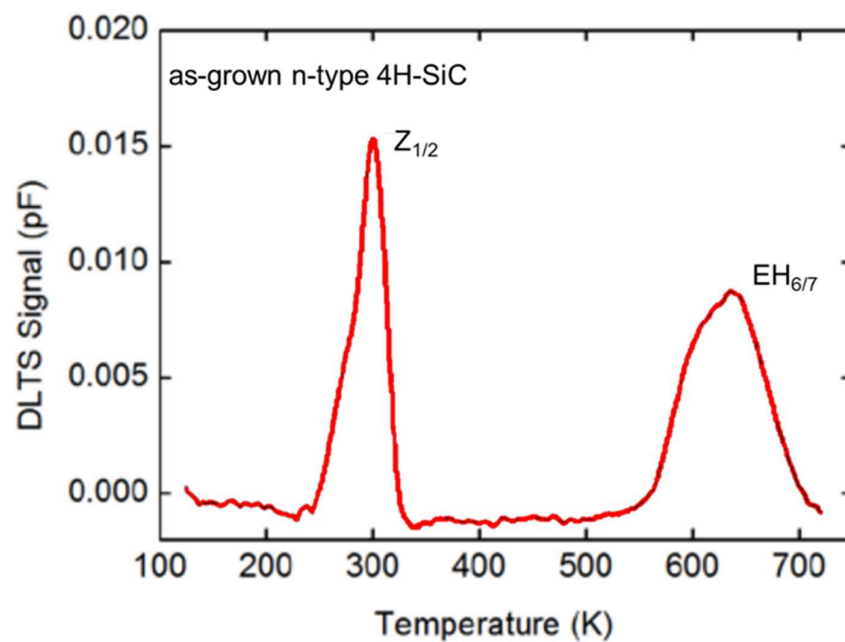


Figure 2. Typical DLTS spectrum for the as grown n-type 4H-SiC sample. Two peaks, Z<sub>1/2</sub> and EH<sub>6/7</sub> are observed.

Son et al. [15] were the first ones who have ascribed Z<sub>1/2</sub> and EH<sub>6/7</sub> to (=/0) and (0/++) transitions from the carbon vacancy, based on the EPR and DLTS measurements. Carbon vacancy (V<sub>c</sub>) is the most dominant defect in 4H-SiC, introduced during the crystal growth and upon irradiation. The V<sub>c</sub> concentration can be increased either by irradiations or high-temperature annealing [12].

As we can see in Figure 2., DLTS peaks are either asymmetric (Z<sub>1/2</sub>, the low temperature side) or very broad (EH<sub>6/7</sub>). From the first studies on Z<sub>1/2</sub> and EH<sub>6/7</sub> it was evident, that the structure behind these defects is not simple. In their pioneering work on Z<sub>1/2</sub> using DLTS, Hemmingsson et al. [19] showed that Z<sub>1/2</sub> is the superposition of two nearly identical Z<sub>1</sub> and Z<sub>2</sub> negative-*U* defect transitions, each located on a different sub-lattice site. However, not until recently, using the L-DLTS, direct evidence that Z<sub>1/2</sub> consists of two components is provided, namely Z<sub>1</sub> and Z<sub>2</sub>, with activation energies for electron emission of 0.59 and 0.67 eV, respectively. These were ascribed to (=/0) transitions of carbon vacancies located at hexagonal and pseudo-cubic sites of the 4H-SiC crystal, respectively [20]. Figure 3.

Shows L-DLTS spectrum for the as-grown 4H-SiC samples. The emission lines arising from the  $Z_{1/2}$  DLTS peak are clearly resolved.

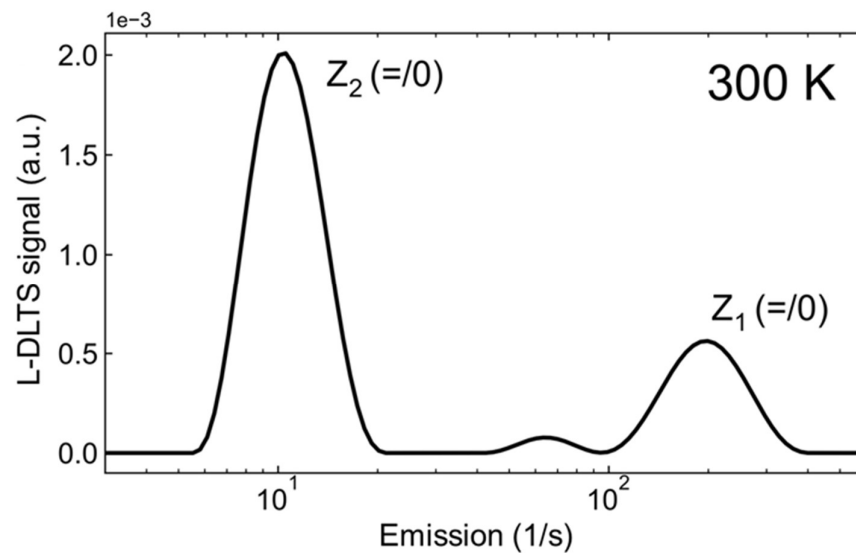


Figure 3. L-DLTS spectrum for the as grown 4H-SiC sample measured at room temperature (RT).

Even before the  $Z_{1/2}$  was resolved by L-DLTS measurements, there were several attempts to resolve the broad  $EH_{6/7}$  peak too. Danno and Kimoto [22] have resolved  $EH_6$  and  $EH_7$  by simulating the Fourier-transform DLTS peak of  $EH_{6/7}$ . The direct evidence that  $EH_{6/7}$  consists of two components was provided by Alfieri and Kimoto [23]. In this study, they have resolved two energy levels at 1.30 and 1.49 eV, for  $EH_6$  and  $EH_7$  respectively.

## 2.2 Silicon Vacancy

Figure 4. shows DLTS spectrum for the 2 MeV He ion implanted n-type 4H-SiC sample. In addition to the  $Z_{1/2}$ , 2 MeV ion implantation has introduced several deep level defects, namely  $S_1$ ,  $S_2$  and  $EH_4$ . In this section we will focus on  $S_1$  and  $S_2$ . Estimated activation energies for electron emission for  $S_1$  and  $S_2$  are 0.40 and 0.70 eV.

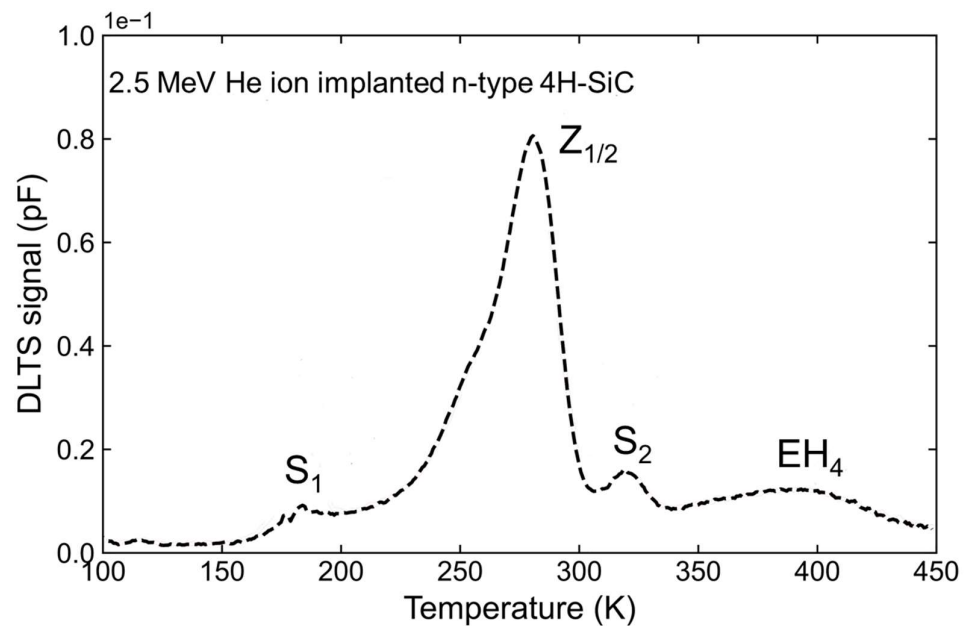


Figure 4. DLTS spectrum for 2 MeV He ion implanted 4H-SiC sample. Several deep level defects are observed: S<sub>1</sub>, Z<sub>1/2</sub>, S<sub>2</sub> and EH<sub>4</sub>.

Deep level defects with those energies have been reported in numerous studies for proton irradiated [1], ion implanted [6], neutron irradiated [18] 4H-SiC samples. The inconsistency in labeling and distinguishing these defects regardless of the particle energy and type used for irradiation has brought confusion while interpreting different published studies. It was evident from all these studies that these levels (0.40 and 0.70 eV) are due to intrinsic defects, interstitials or vacancies. Significant progress in understanding these defects was made by Beathen et al. [1]. They have identified the S<sub>1</sub> and S<sub>2</sub> as V<sub>Si</sub> (-3/=) and V<sub>Si</sub> (=/-) charge states, based on the PL and DLTS measurements, combined with DFT calculations.

Additional progress has been made by L-DLTS measurements. Beathen et al. [1] have shown that S<sub>1</sub> (in proton irradiated samples) has two emission lines arising from V<sub>Si</sub> sitting at  $-k$  and  $-h$  lattice sites. The identical findings have been later confirmed by Brodar et al [18] when studying the fast neutron irradiated 4H-SiC material. Figure 5 shows L-DLTS spectrum for S<sub>1</sub>. The emission line splittings is clearly observed.

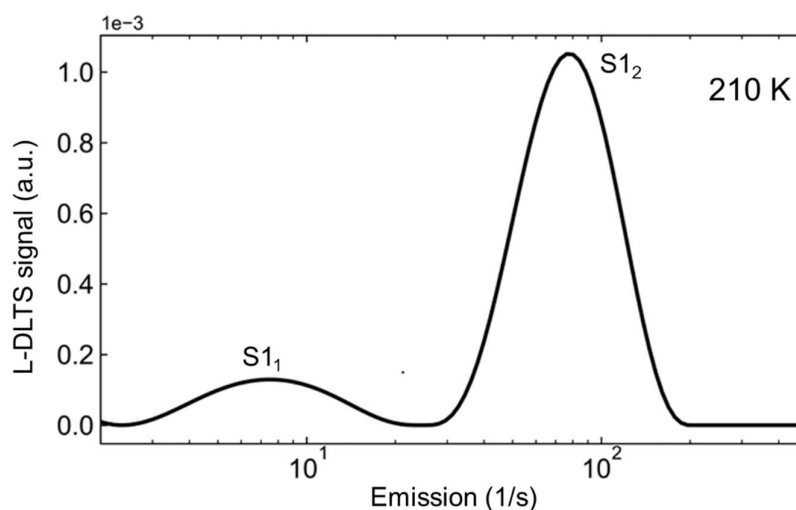


Figure 5. L-DLTS spectrum for 2 MeV He ion implanted 4H-SiC sample measured at 210 K. Data adopted from Ref. [18].

### 2.3. Carbon Interstitial

As already mentioned in the previous section, two energy levels at 0.40 and 0.70 eV have been introduced in 4H-SiC by protons, electrons, neutrons and ions. In order to obtain more information about these defects, and by keeping in mind that the low energy electrons cannot displace silicon atoms (displacement thresholds are 20 eV for C and 35 eV for Si [2]), different studies were performed. Storasta et al. [16] have used low energy electrons to introduce only carbon displacements in the 4H-SiC lattice. They have observed two deep level defects with energies of 0.4 and 0.7 eV, and labeled them as EH<sub>1</sub> and EH<sub>3</sub>. These levels were assigned to a highly mobile defect, such as carbon interstitial.

Alfieri et al. [13] have used the low-energy electrons to introduce carbon displacements only, and then measured activation energies for annealing of the EH<sub>1/3</sub> levels. They have shown that activation energies for annealing of EH<sub>1/3</sub> levels are about 0.7 eV lower than those for S<sub>1/2</sub>(V<sub>Si</sub>), giving strong evidence for distinction of EH- and S-centers.

These studies have led to better understanding of S<sub>1/2</sub> and EH<sub>1/3</sub> defects. It is now evident that these defects can be easily distinguished. While EH<sub>1/3</sub> are introduced by the low-energetic particles (< 150 keV), the S<sub>1/2</sub> deep level defects are introduced by the high-energetic particles.

Recently, Coutinho et al. [24] have reported on M-center (bi-stable defect in 4H-SiC, also introduced by radiation) and identified it as C<sub>i</sub>. M-centre introduces several energy levels which overlap with the already described EH<sub>1/3</sub> and/or S<sub>1/2</sub>, and Z<sub>1/2</sub> deep levels. The relation between the EH<sub>1/3</sub> and M-centre is still unclear.

In addition to above mentioned M-center, Karsthof et al. [25] have introduced excess carbon into n-type 4H-SiC by thermal annealing with a pyrolyzed carbon cap on the sample surface as a carbon source. They have observed several deep level defects, most likely C<sub>i</sub>-related. However, their properties are different from those reported for the M-centre. They have proposed the existence of variety of C<sub>i</sub>-related defects.

It is clear from all the available results that further studies are needed until we reach a full understanding of C<sub>i</sub>-related defects in 4H-SiC.

#### 2.4. Carbon antisite-carbon vacancy pair

The EH<sub>4</sub> and EH<sub>5</sub> are deep level defects commonly found in DLTS spectra of ion implanted or irradiated n-type 4H-SiC samples [6, 14, 18, 21]. The EH<sub>4</sub> has the peak maximum around 400 K (as shown in Figure 4), while the EH<sub>5</sub> appears at slightly higher temperatures. Reported activation energies are around 1.0-1.1 eV below the conduction band.

Karsthof et al. [14] have studied the EH<sub>4</sub> and EH<sub>5</sub> deep level defects by means of DLTS and PL in proton irradiated and subsequently annealed n-type 4H-SiC. They have proposed that the EH<sub>4</sub> (~1.0 eV) and EH<sub>5</sub> (~1.1 eV) originate from the (+/0) charge transition level belonging to different configurations of the carbon antisite-carbon vacancy (C<sub>si</sub>-V<sub>c</sub>) pair.

This result has been additionally confirmed by Nakane et al. [21]. They have used 2 MeV electron irradiation followed by additional annealing, to introduce deep level defects and investigated them by means of photo-induced current transient spectroscopy (PICTS) and EPR. Several deep level defects were introduced. Among them, two deep level defects at energies ~ 0.72 and ~1.07 eV were assigned to (0/-) and (+/0) charge transitions of the C<sub>si</sub>-V<sub>c</sub> pair.

### 3. Conclusions

In this review, we focus on recent advances related to the main radiation induced deep level defects in n-type 4H-SiC. We have provided an overview of the main achievements, mostly based on application of junction spectroscopy techniques. Using the junction spectroscopy techniques, several deep level defects were successfully resolved, e.g., the Z<sub>1</sub> and Z<sub>2</sub>, EH<sub>6</sub> and EH<sub>7</sub>, and S<sub>1</sub>. While significant progress has been achieved for the V<sub>c</sub> and V<sub>Si</sub>, C<sub>i</sub>-related defects are still not yet fully understood.

**Funding:** The present work was financially supported by the NATO Science for Peace and Security Programme, project no. G5674

**Data Availability Statement:** Data is contained within the article.

**Conflicts of Interest:** The author declares no conflict of interest.

### References

1. Bathen, M.E.; Galeckas, A.; Müting, J.; Ayedh, H.M.; Grossner, U.; Coutinho, J.; Frodason, Y.K.; Vines, L. Electrical charge state identification and control for the silicon vacancy in 4H-SiC. *NPJ Quantum Inf.* 2019, 5, 111
2. Kimoto, T.; Cooper, J. A.; (2014). *Fundamentals of Silicon Carbide Technology: Growth, Characterization, Devices, and Applications.* John Wiley & Sons Singapore Pte. Ltd (2014), doi:10.1002/9781118313534

3. Yang, A.; Murata, K.; Miyazawa, T.; Tawara, T.; Tsuchida, H. Analysis of carrier lifetimes in N + B-doped n-type 4H-SiC epilayers. *J. Appl. Phys.* 2019, 126, 055103, <https://doi.org/10.1063/1.5097718>
4. Coutinho, J.; Torres, V.J.B.; Capan, I.; Brodar, T.; Ereš, Z.; Bernat, R.; Radulović, V. Silicon carbide diodes for neutron detection. *Nucl. Inst. Methods Phys. Res. A* 2020, 986, 164793.
5. Peaker, A.R.; Markevich, V.P.; Coutinho, J. Tutorial: Junction spectroscopy techniques and deep-level defects in semiconductors. *J. Appl. Phys.* 2018, 123, 161559.
6. Capan, I.; Brodar, T.; Bernat, R.; Pastuović, Ž.; Makino, T.; Ohshima, T.; Gouveia, J.D.; Coutinho, J. M-center in 4H-SiC: Isothermal DLTS and first principles modeling studies. *J. Appl. Phys.* 2021, 130, 125703
7. Capan, I.; Yamazaki, Y.; Oki, Y.; Brodar, T.; Makino, T.; Ohshima, T. Minority Carrier Trap in n-Type 4H-SiC Schottky Barrier Diodes. *Crystals* 2019, 9, 328. <https://doi.org/10.3390/cryst9070328>
8. David, M.L.; Alfieri, G.; Monakhov, E.M.; Hallén, A.; Blanchard, C.; Svensson, B.G.; Barbot, J.F. Electrically active defects in irradiated 4H-SiC. *J. Appl. Phys.* 2004, 95, 4728–4733.
9. Castaldini, A.; Cavallini, A.; Rigutti, L.; Nava, F.; Ferrero, S.; Giorgis, F. Deep levels by proton and electron irradiation in 4H-SiC. *J. Appl. Phys.* 2005, 98, 053706.
10. Dalibor, T.; Pensl, G.; Kimoto, T.; Matsunami, H.; Sridhara, S.; Devaty, R.P.; Choyke, W.Y. Radiation-induced defect centers in 4H silicon carbide. *Diamond and Related Materials*, 1997 6, 1333-1337.
11. Alfieri, G.; Monakhov, E.V.; Svensson, B.G.; Linnarsson, M.K. Annealing behavior between room temperature and 2000 °C of deep level defects in electron-irradiated n-type 4H silicon carbide. *J. Appl. Phys.* 2005, 98, 043518.
12. Pastuović, Z.; Siegele, R.; Capan, I.; Brodar, I.; Sato, S.; Ohshima, T. Deep level defects in 4H-SiC introduced by ion implantation: The role of single ion regime. *J. Phys. Condens. Matter* 2017, 29, 475701.
13. Alfieri, G.; Mihaila, A. Isothermal annealing study of the EH1 and EH3 levels in n-type 4H-SiC. *J. Phys. Condens. Matter* 2020, 32, 46.
14. Karsthof, R.; Bathen, M.E.; Galeckas, A.; Vines, L. Conversion pathways of primary defects by annealing in proton-irradiated n-type 4H-SiC. *Phys. Rev. B* 2020, 102, 184111.
15. Son, N.T.; Trinh, X.T.; Løvlie, L.S.; Svensson, B.G.; Kawahara, K.; Suda, J.; Kimoto, T.; Umeda, T.; Isoya, J.; Makino, T.; et al. Negative-U System of Carbon Vacancy in 4H-SiC. *Phys. Rev. Lett.* 2012, 109, 187603.
16. Storasta, L.; Bergman, J.P.; Janzén, E.; Henry, A.; Lu, J. Deep levels created by low energy electron irradiation in 4H-SiC. *J. Appl. Phys.* 2004, 96, 4909–4915.
17. David, M.-L.; Alfieri, G.; Monakhov, E.V.; Hallén, A.; Barbot, J.F.; Svensson, B.G. Evidence for Two Charge States of the S-Center in Ion-Implanted 4H-SiC. *Mater. Sci. Forum* 2003, 433–436, 371–374.

18. Capan, I.; Brodar, T.; Makino, T.; Radulovic, V.; Snoj, L. M-Center in Neutron-Irradiated 4H-SiC. *Crystals* 2021, 11, 1404. <https://doi.org/10.3390/cryst11111404>
19. Hemmingsson, C.G.; Son, N.T.; Ellison A.; Zhang, J.; Janzén, E.. Negative- U centers in 4 H silicon carbide. *Phys. Rev. B.* 58 (1998) R10119–R10122. doi:10.1103/PhysRevB.58.R10119.
20. Capan, I.; Brodar, T.; Coutinho, J.; Ohshima, T.; Markevich, V.P.; Peaker, A.R. Acceptor levels of the carbon vacancy in 4 H -SiC: Combining Laplace deep level transient spectroscopy with density functional modeling. *J. Appl. Phys.* 2018, 124, 245701.
21. Nakane, H.; Kato, M.; Ohkouchi, Y.; Trinh, X.T.; Ivanov, I.G.; Ohshima, T.; Son, N.T. Deep levels related to the carbon antisite–vacancy pair in 4H-SiC. *J. Appl. Phys.* 2021, 130, 065703.
22. Danno, K.; Kimoto, T. Investigation of deep levels in *n*-type 4H-SiC epilayers irradiated with low-energy electrons. *J. Appl. Phys.* 2006, 100, 113728.
23. Alfieri, G.; Kimoto, T. Resolving the *EH6/7EH6/7* level in 4H-SiC by Laplace-transform deep level transient spectroscopy. *Appl. Phys. Lett.* 2013, 102, 152108.
24. Coutinho, J.; Gouveia, J.D.; Makino, T.; Ohshima, T.; Pastuović, Ž.; Bakrač, L.; Brodar, T.; Capan, I. M center in 4H-SiC is a carbon self-interstitial. *Phys. Rev. B* 2021, 103, L180102.
25. Karsthof, K.; Bathen, M.E.; Kuznetsov, A.; Vines, L. Formation of carbon interstitial-related defect levels by thermal injection of carbon into *n*-type 4H-SiC. *J. Appl. Phys.* 2022, 131, 035702.